Inorganic Chemistry

Article

pubs.acs.org/IC

Interplay between Organic−Organometallic Electrophores within Bis(cyclopentadienyl)Molybdenum Dithiolene Tetrathiafulvalene Complexes

Nathalie Bellec, Antoine Vacher, Frédéric Barrière, Zijun Xu, Thierry Roisnel, and Dominique Lorcy*

Institut des Sciences Chimiques de Rennes, UMR 6226 CNRS-Université de Rennes 1, Campus de Beaulieu, Bât 10A, 35042 Rennes cedex, France

Supporting Information

ABSTRACT: Tetrathiafulvalenes (TTF) and bis(cyclopentadienyl) molybdenum dithiolene complexes, Cp_2Mo(dithiolene) complexes, are known separately to act as good electron donor molecules. For an investigation of the interaction between both electrophores, two types of complexes were synthesized and characterized. The first type has one Cp_2Mo fragment coordinated to one TTF dithiolate ligand, and the second type has one TTF bis(dithiolate) bridging two Cp_2Mo fragments. Comparisons of the electrochemical properties of these complexes with those of models of each separate electrophore provide evidence for their mutual influence. All of these complexes act as very good electron donors with a first oxidation potential 430 mV lower than the tetrakis(methylthio)TTF. DFT calculations suggest that the HOMO of the neutral complex and the SOMO of the cation are delocalized across the whole TTF dithiolate ligand. The X-ray crystal structure analyses of the neutral and the mono-oxidized Cp_2Mo(dithiolene)(bismethylthio)TTF complexes are consistent with the delocalized assignment of the highest occupied frontier molecular orbitals. UV−vis−NIR spectroelectrochemical investigations confirm this electronic delocalization within the TTF dithiolate ligand.

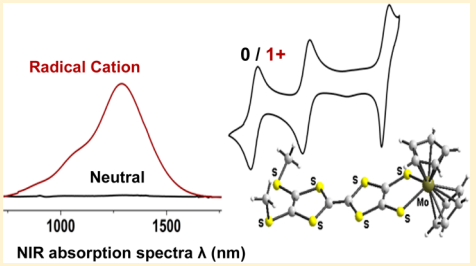

INTRODUCTION

Over the past decades, metal 1,2-dithiolene complexes with tetrathiafulvalene (TTF) dithiolate ligands have regained attention due to the exceptional conducting properties found in some of these complexes.[1] For instance, single component molecular conductors were obtained when two TTF dithiolate ligands were coordinated to various metals.[2−4] On one hand, the TTF is a redox active core which can be easily oxidized sequentially to the cation radical and dicationic state. On the other hand, a dithiolene ligand, which is known as a non-innocent ligand,[5] is also electroactive as it can be reversibly oxidized to the radical anion and the neutral thioketone state. Moreover, metal bis(1,2-dithiolene) complexes, depending on different parameters (the substituents, the metal, and the redox states), can behave as strong NIR absorbers.[6] Contrary to these homoleptic dithiolene complexes, heteroleptic ones such as mixed bis(cyclopentadienyl)/dithiolene metal complexes with one TTF dithiolate ligand, $Cp_2M(S_2TTF)$, have been scarcely studied as only a few examples with M = Ti,[7,8] Zr,[9] and Hf[9] have been reported so far (Chart 1). Some of these oxidized heteroleptic complexes exhibit semiconducting behavior, and calculations show that the spin is essentially located on the TTF core within these complexes.[3]

The series of the titanocene dithiolene complexes is the only case where either a TTF dithiolate ligand has been coordinated to a Cp_2Ti fragment or a TTF tetrathiolate has been coordinated to two Cp_2Ti fragments. One characteristic of these d^0, 16 e^-, Cp_2Ti(dithiolene) complexes is that an irreversible

Chart 1

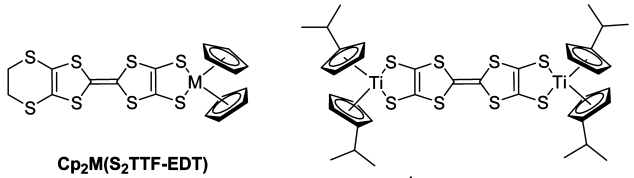

electrochemical oxidation of the metallacycle process is observed due to the decoordination of the oxidized ligand from the Cp_2Ti moiety.[10,11] Indeed, the removal of one electron from the HOMO severely weakens the metal−ligand interactions.[12] Contrariwise, Cp_2Mo(dithiolene) complexes, which are electron rich d^2, 18 e^- complexes, can be oxidized reversibly into cation radical species.[13,14] It would be therefore attractive to link together these two efficient electrophores, TTF on one hand, and the Cp_2Mo(dithiolene) moiety on the other hand. To the best of our knowledge, no example of such a molybdocene complex involving TTF dithiolate ligand has been described, while the corresponding Cp_2Mo(dmit) (dmit = 1,3-dithiole-2-thione-4,5-dithiolate) is known to lead to various cation radical species which form crystalline magnetic molecular materials.[13a,15] Accordingly, we decided to investigate the

Received: March 19, 2015
Published: April 30, 2015

DOI: 10.1021/acs.inorgchem.5b00632
Inorg. Chem. 2015, 54, 5013−5020

synthesis of Cp_2Mo(dithiolene) complexes where one TTF dithiolate ligand is coordinated to one Cp_2Mo fragment, $Cp_2Mo(S_2TTF(SR)_2)$ **2a,b**, and where two Cp_2Mo fragments are bridged by one TTF bis(dithiolate), $(Cp_2Mo)_2(S_4TTF)$, **4** (Chart 2). Herein, we report the synthesis of these complexes

Chart 2

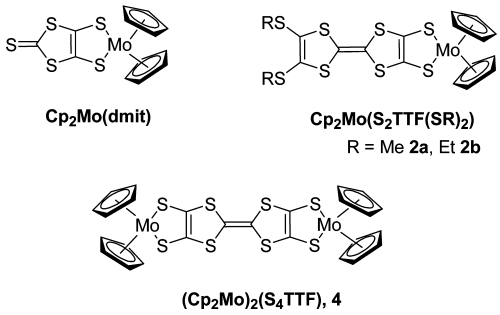

together with their structural, electrochemical, and spectro-electrochemical properties. These investigations show sizable interactions between the TTF core and the organometallic fragment Cp_2Mo, and these results are also supported by DFT calculations.

RESULTS AND DISCUSSION

Synthesis and Electrochemical Properties. The target compounds were prepared starting from TTFs **1a,b**[16] and **3**[16] according to the chemical pathway depicted in Scheme 1.

Scheme 1

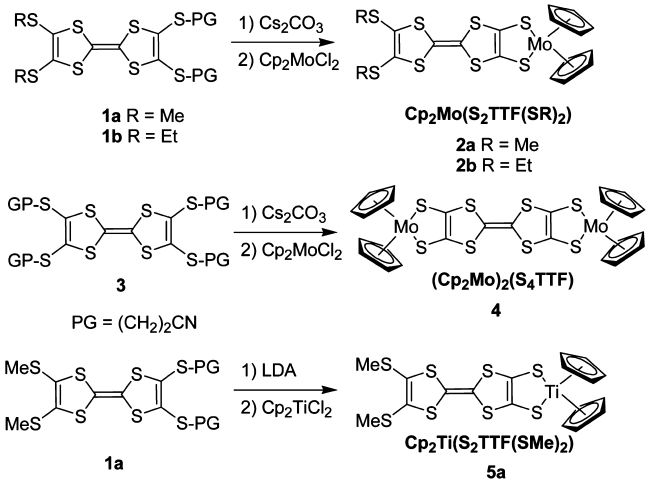

These TTFs, **1a,b** and **3**, are the cyanoethyl protected forms of the TTF dithiolates and TTF tetrathiolate, respectively, which are easily generated in a basic medium. Treatment of TTF **1a,b** with 2.5 equiv of cesium carbonate, Cs_2CO_3, followed by the addition of Cp_2MoCl_2 leads to the desired TTF **2a,b** in 64% and 52% yield, respectively. Similarly, the addition of an excess of Cs_2CO_3 to a solution of TTF **3** affords the TTF tetrathiolate, which reacts with 2 equiv of Cp_2MoCl_2 to give the corresponding TTF **4**, $(Cp_2Mo)_2(S_4TTF)$, which precipitates in the medium. This TTF **4** is poorly soluble in dichloromethane. The titanium complex analogue of **2a**, $Cp_2Ti(S_2TTF(SMe)_2)$ **5a**, was also synthesized according to similar experimental conditions using Cp_2TiCl_2 as reactant, in order to examine and compare the influence of the metal on the overall properties.

Crystals suitable for X-ray structure analysis were obtained for complexes **2a** and **5a**. These compounds crystallize in the monoclinic system, space goup $P2_1/n$ for both. The molecular structures of **2a** and **5a** are presented in Figure 1, and selected bond lengths and angles are listed in Table 1 together with those of $Cp_2Mo(dmit)$[13b] and $Cp_2Ti(dmit)$[10] for comparison.

Within complex **2a**, the TTF core is not planar and exhibits a boat conformation, with the dithiole rings folded along the S···S vectors with values of 17.9(1)° and 20.1(2)° for S3···S4 and S5···S6, respectively. The central C13═C14 bond of 1.346(6) Å is typical for neutral TTF. The MoS_2C_2 metallacycle is nearly planar with a folding angle θ of 2.92(9)° close to that observed in $Cp_2Mo(dmit)$.[15d] The bond lengths and bond angles of this metallacycle are in the range of those found for the $Cp_2Mo(dmit)$ (Table 1). For the titanocene complex **5a**, the TTF core exhibits also a boat conformation, with the dithiole rings folded along the S···S vectors with values of 26.54(8)° and 20.06(8)° for S3···S4 and S5···S6, respectively. The main difference between the two complexes **2a** versus **5a** lies on the metallacycle which is severely distorted in the case of the titanocene derivative **5a** along the S···S axis with a folding angle θ of 47.95(48)°, a recurrent characteristic of these 16 e^- complexes.[13b,10] As a consequence, the ^1H NMR spectra of **2a** and **5a** in $CDCl_3$ are also different: for **5a** the two Cp rings are not equivalent, and two singlets are observed while for **2a** only one signal for the two Cp rings is observed.[13b] In the solid state, both complexes are arranged in a head-to-tail fashion with the shortest S···S intermolecular contact being equal to 3.652(2) Å for **2a** and 3.585(1) Å for **5a**, while the shortest C···C intermolecular contact amounts to 3.338(7) Å for **2a** (C13/C13) and 3.288(3) Å for **5a** (C14/C14).

The redox properties of complexes **2a,b** and **4** were analyzed by cyclic voltammetry performed in CH_2Cl_2 for **2a,b** and in $DMSO/CH_2Cl_2$ (1/8) for **4** containing 0.1 M of Bu_4NPF_6 as supporting electrolyte. The oxidation potentials are collected in Table 2 together with those of the Cp_2Ti complex analogue **5a** for comparison.

For the three complexes **2a,b** and **4**, three reversible oxidation waves can be observed on the voltammograms. In the case of **2a,b**, these three redox processes are monoelectronic, as shown in Figure 2 for **2a**, indicating the stepwise formation of four redox states from the neutral to the trication species $\mathbf{2}^{3+}$. For **4** the first two waves are also monoelectronic. The third wave displays an anodic peak current intensity (I_{pa}) slightly higher than those of the first two. However, as it occurs at the limit of the available potential window of the medium it is rather difficult to determine if it is a two-electron process involving both Cp_2Mo(dithiolene) centers. The first two redox processes observed for complexes **2a,b** and **4** are tentatively assigned to the sequential oxidation of the TTF core into the cation radical and the dication species. Interestingly, if we compare the first oxidation potentials with those of the tetrathiomethyl-TTF, $TTF(SMe)_4$, the first redox process occurs at significantly lower anodic potentials (**2a,b** E_{ox}^1 = 0.06−0.05 V and $TTF(SMe)_4$ E_{ox}^1 = 0.49 V vs SCE). This behavior is reminiscent of what was previously observed for other complexes such as the ruthenium-acetylide-tetrathiafulvalene complex,[17] *trans*-[RuCl(C≡CMe_3TTF)], where the metal−organic electrophores are strongly electronically coupled and where an increase of the electron density on the TTF from the metal fragment was efficiently transmitted by the acetylide linker. It is also interesting to compare the effect of the nature of the metal on the redox properties of these complexes.

DOI: 10.1021/acs.inorgchem.5b00632
Inorg. Chem. 2015, 54, 5013−5020

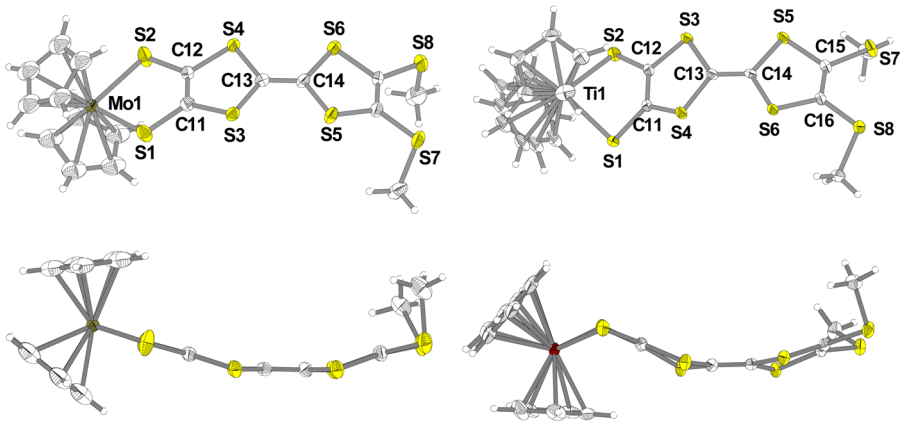

Figure 1. Perspective views of $Cp_2Mo(S_2TTF(SMe)_2)$ **2a** (top left) and $Cp_2Ti(S_2TTF(SMe)_2)$ **5a** (top right) with the atom labeling and their side views (bottom). Thermal ellipsoids are shown at a 50% probability level.

Table 1. Bond Lengths (Å) and Angles (deg) of the Metallacycle for Complexes 2a, 5a, $Cp_2Mo(dmit)$,[15d] and $Cp_2Ti(dmit)$[10]

	M—S	C—S	C=C	Θ
2a	2.464(2)	1.749(4)	1.332(5)	2.92(9)
	2.461(1)	1.751(4)		
$Cp_2Mo(dmit)$	2.457(3)	1.745(9)	1.357(12)	4.2(1)
5a	2.444(1)	1.723(2)	1.370(3)	47.95(5)
	2.420(1)	1.727(2)		
$Cp_2Ti(dmit)$	2.431(2)	1.72(1)	1.357(15)	47.4(3)

Table 2. Redox Potentials[b] of Complexes 2a,b, 4, 5a, and $Cp_2Mo(dmit)$ (E in V vs SCE)

compound	E_{red}	E_{ox}^1 (ΔE_p)	E_{ox}^2 (ΔE_p)	E_{ox}^3 (ΔE_p)
2a	−1.10[a]	0.06 (60)	0.52 (60)	1.26 (60)
2b	−1.14[a]	0.05 (60)	0.53 (70)	1.27 (70)
4	−0.90[a]	−0.16 (60)	0.18 (60)	0.76 (90)
$TTF(SMe)_4$		0.49 (80)	0.83 (80)	
$Cp_2Mo(dmit)$[18]		0.39	1.03	
5a	−0.99 (70)	0.39 (80)	0.71 (145)	0.99 (110)

[a]Irreversible process. [b]Oxidation processes, taken as the average of the anodic and the cathodic peak potentials; ΔE_p represents peak-to-peak separation.

Indeed, when switching from Mo in **2a** to Ti in **5a** an important anodic shift of 330 mV is observed as the first oxidation process occurs at E_{ox}^1 = 0.39 V versus SCE. The third oxidation system in **2a,b** and **4** is then logically viewed as involving the Cp_2Mo(dithiolene) moieties. Compared with the first oxidation potential of $Cp_2Mo(dmit)$ (E_{ox}^1 = 0.39 V vs SCE), this oxidation process in **2a,b** (E_{ox}^3 = 1.26 V vs SCE), analyzed in the same experimental conditions, is anodically shifted by 870 mV. This could be explained by the presence of the TTF dication acting now as a strong electron acceptor. On the cathodic scan, all these complexes exhibit one reduction wave which is reversible in the case of **5a** and irreversible for the Mo complexes **2a,b** and **4** (Table 2), consistent with the calculated nature of the LUMO (*vide infra*). This reduction process corresponds to the reduction of the metal $Ti^{(IV)}/Ti^{(III)}$ for **5a** and $Mo^{(IV)}/Mo^{(III)}$ for **2a**−**b** and **4**.

Ion Radical Salts of 2a. The low oxidation potentials of $Cp_2Mo(S_2TTF(SMe)_2)$ **2a** and its solubility into organic solvents open the possibility to form charge transfer salts with an organic acceptor such as TCNQ which is reduced at 0.18 V versus SCE. A salt was indeed obtained by simply mixing a solution of the molybdenum complex **2a** in CH_2Cl_2 with a solution of TCNQ in CH_3CN. The charge transfer salt precipitates immediately from the solution as deep violet powder which proved to be insoluble in organic solvents. Elemental analysis reveals a 1:1 stoichiometry with 1 complex **2a** for 1

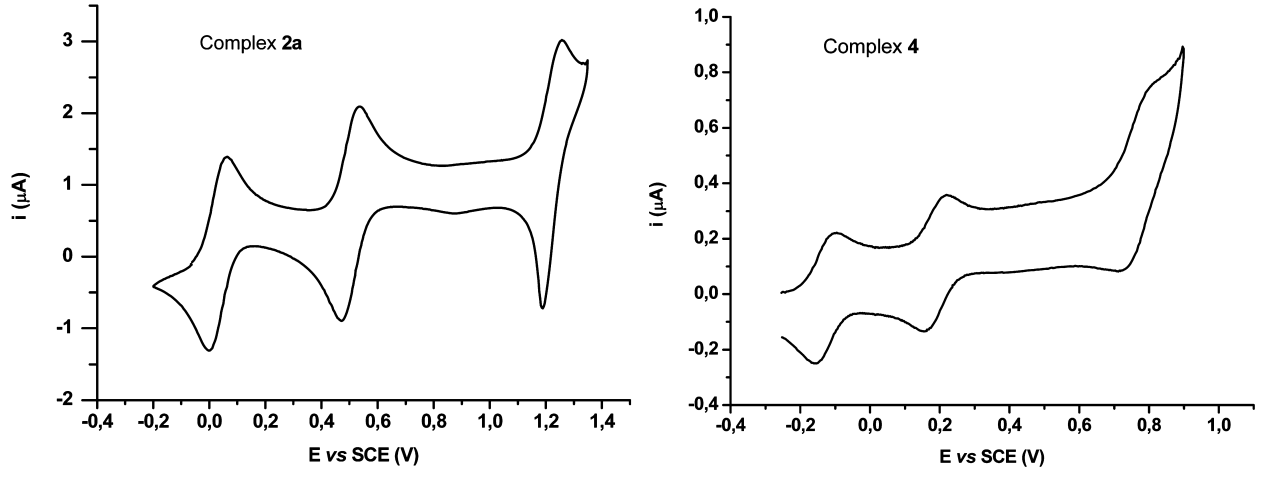

Figure 2. Cyclic voltammograms of **2a** (left) in CH_2Cl_2 and **4** (right) in DMSO/CH_2Cl_2 (1/8), 100 mV/s, Bu_4NPF_6 0.1 M.

DOI: 10.1021/acs.inorgchem.5b00632
Inorg. Chem. 2015, 54, 5013−5020

Table 3. Selected Experimental and Calculated Bond Lengths (Å) for 2a and $2a^{\bullet+}$ (M = Mo) and 5a (M = Ti)

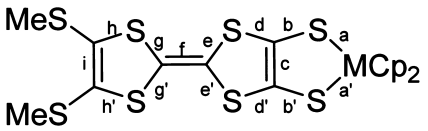

bonds	2a	2a calcd	$2a^{\bullet+}$	$2a^{\bullet+}$ calcd	5a	5a calcd	$5a^{\bullet+}$ calcd
a	2.4613(12)	2.510	2.4599(14)	2.544	2.444(1)	2.482	2.516
a′	2.4639(12)	2.510	2.4640(14)	2.547	2.420(1)	2.494	2.533
b	1.749(4)	1.819	1.712(5)	1.791	1.723(2)	1.792	1.780
b′	1.751(4)	1.819	1.715(6)	1.790	1.727(2)	1.793	1.778
c	1.332(6)	1.347	1.394(7)	1.381	1.370(3)	1.375	1.393
d	1.765(4)	1.841	1.736(5)	1.811	1.762(3)	1.835	1.816
d′	1.759(4)	1.840	1.732(5)	1.812	1.765(2)	1.836	1.817
e	1.761(4)	1.844	1.731(6)	1.821	1.761(3)	1.843	1.811
e′	1.759(4)	1.845	1.737(5)	1.821	1.760(2)	1.843	1.811
f	1.346(6)	1.348	1.385(7)	1.369	1.340(3)	1.348	1.378
g	1.761(4)	1.844	1.734(5)	1.821	1.757(3)	1.845	1.813
g′	1.760(4)	1.847	1.729(5)	1.821	1.758(3)	1.843	1.813
h	1.757(4)	1.847	1.745(6)	1.840	1.767(2)	1.841	1.836
h′	1.760(4)	1.842	1.758(5)	1.839	1.759(2)	1.845	1.836
i	1.342(6)	1.354	1.353(7)	1.356	1.349(3)	1.354	1.358

TCNQ. The degree of charge transfer between the donor and the acceptor was inferred from analysis of the nitrile stretching absorption band in the FTIR spectrum. The nitrile vibration band observed for this salt was found at ν_{CN} = 2170 cm^{-1} which is close to the energy value reported for $TCNQ^{-1}$ (ν_{CN} = 2185 cm^{-1}) in its NaTCNQ salt.[19] Therefore, from this analysis, a charge close to −1 was found for the TCNQ indicating that the complex obtained is under the cation radical form, $2a^{\bullet+}$. Due to its low solubility no further investigations could be performed on [2a][TCNQ].

Oxidation of **2a**, $Cp_2Mo(S_2TTF(SMe)_2)$, was also realized with iodine in CH_2Cl_2. Crystals suitable for X-ray diffraction studies were obtained by recrystallization of the precipitate in acetonitrile. This salt crystallizes in the triclinic system, space group $P\bar{1}$. Crystal structure determination reveals a 1:1 stoichiometry with one $Cp_2Mo(S_2TTF(SMe)_2)$ **2a** for one I_3^-, [2a][I_3], indicating that the complex is under the cation radical state, $2a^{\bullet+}$. Bond lengths and bond angles of the donor skeleton are collected in Table 3. The molecular structure of $2a^{\bullet+}$, reported in Figure 3, shows that within this oxidized

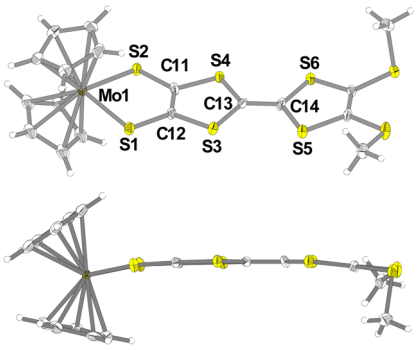

Figure 3. Perspective view of the complex $2a^{\bullet+}$ in [2a][I_3] (top) and its side view (bottom). Thermal ellipsoids are shown at a 50% probability level.

complex the TTF core is now planarized, as the folding angles along the S···S vectors amount to 0.7(3)° and 6.1(2)° for S3···S4 and S5···S6, respectively. Comparison of the geometrical characteristics between the neutral and the cation radical states of the complex **2a** allowed us to analyze the modifications occurring upon oxidation. For instance, on the metallacycle, the folding angle θ along the S1···S2 is slightly increased as it amounts to 8.5(1)°.

Comparison of the bond lengths between the neutral and the cation radical state of complex **2a** (Table 3) shows several modifications which occur on the TTF core itself and also on the dithiolene moiety. For the TTF core, a lengthening of the central C═C bond is observed as well as a shortening of all the C—S bonds of the dithiole rings. These modifications are usually observed when going from the neutral state to the cation radical state of the TTF.[20] Concomitantly, the metallacycle itself is also subject to bond length and bond angle modifications upon oxidation. For instance, the C—S bonds are shortened while the C═C bond is lengthened as also observed between neutral and mono-oxidized molybdenum dithiolene complexes.[15,18] On these grounds, the first oxidation of **2a** is suggested to be centered on the TTF core with some delocalization toward the dithiolene-molybdenum center.

In the solid state, the radical cations $2a^{\bullet+}$ form dimers with a head to tail organization (Figure 4). Several short S···S intermolecular contacts along the *a* axis between the neighboring dimers and face-to-face Cp···Cp contacts between neighboring radical cations $2a^{\bullet+}$, with the shortest C···C distance of 3.171(9) Å, can be observed. Note also, within the dimers, the presence of the shortest S···S intermolecular contacts, between the S atom of the neighboring dithiole rings (3.507(6) and 3.518(6) Å) and a short C14···C14 intermolecular contact (3.228(8) Å). This overlap geometry is well-known to lead to a strong antiferromagnetic pairing of the radical species of the TTFs. This analysis is confirmed by the magnetic susceptibility which exhibits no paramagnetism in the whole temperature range (5−300 K). In order to confirm the presence of radical species within this salt, we also investigated [2a][I_3] in solution by EPR spectroscopy. The EPR spectrum of [2a][I_3] was recorded in acetonitrile at room temperature. A single line at a *g* factor of 2.0097 consistent with the presence of TTF radical species is observed.

DOI: 10.1021/acs.inorgchem.5b00632
Inorg. Chem. 2015, 54, 5013−5020

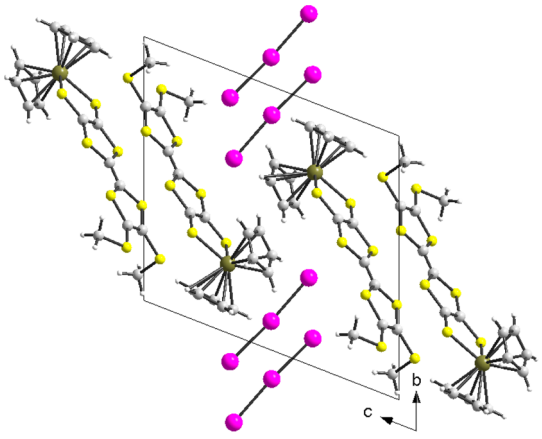

Figure 4. View of the unit cell along the *bc* plane of [**2a**][I_3].

Spectroscopic Properties. UV−vis−NIR investigations were carried out on complexes **2a** and [**2a**][I_3] in a CH_2Cl_2 solution. As illustrated in Figure 5, the neutral complex exhibits

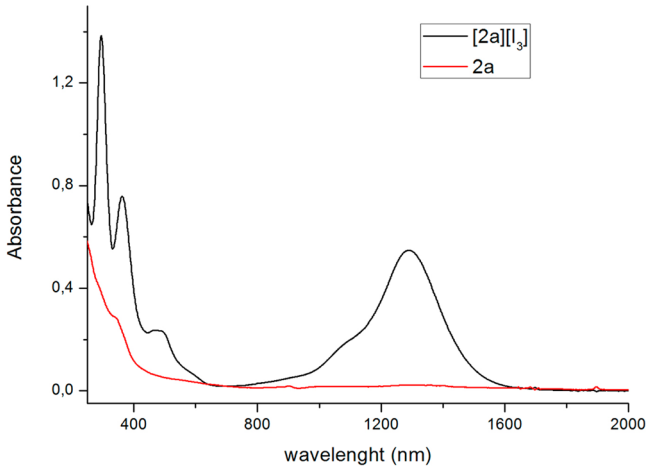

Figure 5. Absorption spectra of complex **2a** ($c = 5 \times 10^{-5}$ M) and [**2a**][I_3] ($c = 2 \times 10^{-5}$ M) in CH_2Cl_2.

absorption bands only in the UV−vis range close to those observed for other Cp_2Mo(dithiolene) complexes. For [**2a**][I_3], besides the bands in the UV−vis range at λ_{max} = 291, 359, and 480 nm, a broad absorption band in the NIR range at λ_{max} = 1081 and 1287 nm results from the combination of two transitions. The spectrum of **2a**$^{\bullet+}$ is clearly different from the spectrum of $TTF(SMe)_4^{\bullet+}$ where the lowest energy transitions were found at about 873 and 458−484 nm.[21] This difference highlights the effect of the Cp_2Mo(dithiolene) fragment on the TTF core.

The UV−vis−NIR spectroelectrochemical investigation was also carried out on the more soluble complex **2b** in CH_2Cl_2 containing 0.2 M Bu_4NPF_6. The spectrum of the neutral complex **2b** is very close to that of **2a** and exhibits absorption bands in the UV−vis range. The spectrum evolution upon oxidation of complex **2b** is reported in Figure 6. Upon gradual oxidation to the mono-oxidized species, **2b**$^{\bullet+}$, the growth of two broad bands in the NIR region centered at 1083 and 1290 nm together with a weaker band centered at 450 nm is observed. The spectrum of complex **2b**$^{\bullet+}$ displays common features with complex **2a**$^{\bullet+}$ in [**2a**][I_3]. Upon oxidation to the bis-oxidized species, **2b**$^{2+}$, these two bands disappear at the expense of two

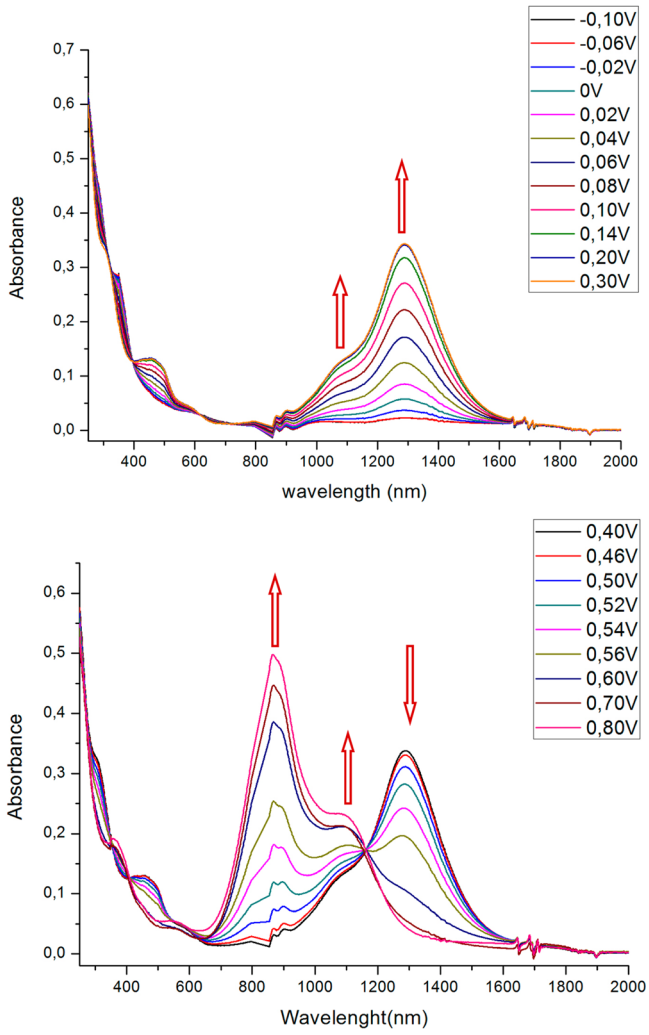

Figure 6. UV−vis−NIR absorption spectra monitoring from −0.10 to 0.30 V (top) and from 0.40 to 0.80 V (bottom) of the electrochemical oxidation of **2b** in CH_2Cl_2 containing 0.2 M Bu_4NPF_6.

new bands that grow at higher energy, 879 and 1092 nm, together with the disappearance of the band centered at 450 nm.

DFT Computational Studies. Geometry optimizations were carried out on the Mo complex **2a** and the Ti complex **5a** for comparison (DFT, Gaussian09, B3LYP/LanL2DZ). The optimized geometries are in good agreement with the structures determined by X-ray diffraction studies, with a boat-like conformation of the TTF core in the neutral complex **2a** and an almost planar TTF core in the mono-oxidized species **2a**$^{\bullet+}$ (Figures 7 and 8). As shown in Figure 7, the HOMO of **2a** is found mainly localized on the TTF dithiolate ligand. Contrariwise the HOMO of $Cp_2Ti(S_2TTF(SMe)_2)$ is mainly localized on the TTF core. The calculated energy of the HOMO of **2a** (−4.48 eV) lies at a significantly higher energy (0.51 or 0.56 eV higher, respectively) than either the HOMO of the Ti analogue **5a** (−4.99 eV) or the HOMO of Cp_2Mo(dmit) (−5.04 eV)[18] in accordance with their redox data (*vide supra*). The LUMOs, for **2a** (−2.42 eV), Cp_2Mo(dmit) (−2.58 eV),[18] and **5a** (−3.00 eV), are centered on the Cp_2M moiety (M = Mo, Ti). In the mono-oxidized state (Figure 8), it can be noticed that the SOMO of **2a**$^{\bullet+}$ is found to have a pronounced TTF dithiolate character, while for **5a**$^{\bullet+}$ there is also a contribution from the metal. Actually, it was already observed in molybdocene that in the

DOI: 10.1021/acs.inorgchem.5b00632
Inorg. Chem. 2015, 54, 5013−5020

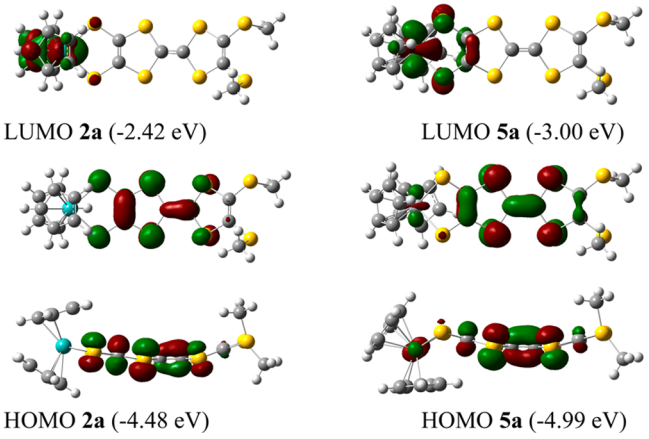

Figure 7. Frontier molecular orbitals (top and side view of HOMOs and top view of LUMOs) shown with a cutoff of 0.04 $[e/bohr^3]^{1/2}$ and calculated energy levels for **2a** (left) and **5a** (right).

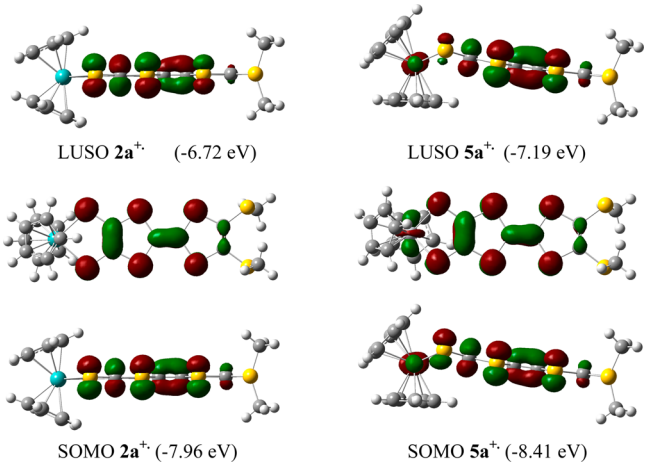

Figure 8. Frontier molecular orbitals (top and side view of SOMOs and side view of LUSOs) shown with a cutoff of 0.04 $[e/bohr^3]^{1/2}$ and calculated energy levels for $\mathbf{2a}^{\bullet+}$ (left) and $\mathbf{5a}^{\bullet+}$ (right).

presence of electron rich dithiolene ligand the spin density is mostly centered on the dithiolene ligand with no contribution of the metal. Usually, this type of Cp_2Mo(dithiolene) complex also presents an unfolded structure along the S···S hinge of the metallacycle associated with an absence of mixing of the Cp_2Mo and dithiolene frontier orbitals. This is consistent with the assignment of the first and second oxidation of **2a** as redox processes centered on the TTF dithiolate moiety.

The calculated bond lengths of complexes **2a**, $\mathbf{2a}^{\bullet+}$, **5a**, and $\mathbf{5a}^{\bullet+}$ in their optimized geometries are reported in Table 3 together with the distances determined by the X-ray diffraction study of **2a**, $\mathbf{2a}^{\bullet+}$, and **5a**. The calculated bond lengths of **2a**, **5a**, and $\mathbf{2a}^{\bullet+}$ are slightly longer than those obtained by X-ray except for the central C═C bond of the TTF and the C═C bond of the metallacycle of $\mathbf{2a}^{\bullet+}$ which were observed to be longer in the X-ray diffraction study (Table 3). Nevertheless, similar trends between the neutral and the oxidized species can be observed in the calculated geometries. Indeed, both the TTF core (lengthening of the central C═C bond and shortening of all the C—S bonds) and the metallacycle (shortening of the C—S bonds) are subject to bond length modifications.

CONCLUSION

Cp_2Mo(dithiolene) complexes formed with TTF dithiolate ligands were prepared and characterized. Electrochemical investigations of these derivatives show that the vicinity of the two electrophores leads to complexes with higher electron donating ability than that of the isolated electrophores, namely, $TTF(SMe)_4$ and Cp_2Mo(dmit). UV−vis−NIR spectroscopic investigations carried out on the neutral and mono-oxidized species as well as UV−vis−NIR spectroelectrochemical analyses have provided evidence for the interplay between the two closely joined electrophores. This indicates an electronic delocalization across the whole TTF dithiolene backbone that was also supported by comparison of the crystal structure of the neutral with that of the oxidized species of $Cp_2Mo(S_2TTF(SMe)_2)$ and was confirmed with DFT modeling.

EXPERIMENTAL SECTION

TTFs **1a,b** and **3** were synthesized according to literature procedure.[16] ^1H NMR spectra were recorded on a Bruker AV300III spectrometer, and chemical shifts are quoted in parts per million (ppm) referenced to tetramethylsilane. Melting points were measured on a Kofler hot-stage apparatus and are uncorrected. Mass spectra were recorded with Waters Q-Tof 2 and Bruker MaXis 4G instruments by the Centre Régional de Mesures Physiques de l'Ouest, Rennes. Column chromatography was performed using Merck 60 silica gel (70−260 mesh). Cyclic voltammetry was carried out in CH_2Cl_2 for **2a,b** and in DMSO/CH_2Cl_2 1/8 for **4**, containing 0.1 M nBu_4NPF_6 as supporting electrolyte. Voltammograms were recorded at 0.1 V s^{-1} on a platinum electrode, and the potentials were measured versus saturated calomel electrode (SCE). The spectroelectrochemical setup was referenced versus SCE in CH_2Cl_2 containing 0.2 M Bu_4NPF_6. A Cary 5000 spectrophotometer was employed to record the UV−vis−NIR spectra. The EPR measurements were performed on Bruker ESP-300E X-band spectrometer. The EPR study was carried out on a CH_3CN solution of $[\mathbf{2a}][I_3]$.

Synthesis of $Cp_2Mo(S_2TTF(SR)_2)$ 2a (R = Me) and 2b (R = Et). To a solution of TTF **1** (233 mg for **1a** and 247 mg for **1b**, 0.5 mmol) in 20 mL of DMF was added, under argon, a solution of cesium carbonate (410 mg, 1.25 mmol) in 15 mL of methanol. The solution was stirred 30 min at room temperature (RT) and 5 min at 60 °C to complete the deprotection. After the reaction mixture was cooled, neat Cp_2MoCl_2 (150 mg, 0.5 mmol) was added, and the reaction was heated at 80 °C for 2 h and stirred overnight at RT. The reaction mixture was filtrated, and the filtrate was evaporated to dryness. The solid was washed with methanol and filtrated under vacuum to give dithiolene complexes **2a,b** as dark brown solids which were crystallized by slow concentration of a dichloromethane solution. Data for **2a**, R = CH_3, follow: yield = 64%, mp = 210 °C; ^1H NMR (300 MHz, $CDCl_3$) δ = 2.39 (s, 6H, SCH_3), 5.36 (s, 10H, Cp); HRMS (ESI) calculated for $C_{18}H_{16}S_8{}^{98}Mo$, 585.80718, found 585.8062. Data for **2b**, R = Et, follow: yield = 52%; mp = 230 °C; ^1H NMR (300 MHz, $CDCl_3$) δ = 1.28 (t, 6H, CH_3), 2.81 (q, 4H, SCH_2), 5.37 (s, 10H, Cp); HRMS (ESI) calculated for $C_{20}H_{20}S_8{}^{98}Mo$, 613.83848, found 613.8372.

Synthesis of $(Cp_2Mo)_2(S_4TTF)$ 4. To a solution of TTF **3** (136 mg, 0.25 mmol) in 20 mL of DMF was added, under argon, a solution of cesium carbonate (410 mg, 1.25 mmol) in 15 mL of methanol. The solution was stirred 30 min at RT and 5 min at 60 °C to complete the deprotection. After the reaction mixture was cooled, neat Cp_2MoCl_2 (150 mg, 0.5 mmol) was added, and the reaction was heated at 80 °C for 2 h and stirred overnight at RT. The reaction mixture was filtrated to give 114 mg of dithiolene complex **4** as a black solid. The filtrate was evaporated to dryness, and compound **4** was washed with methanol and filtrated under vacuum to give 68 mg of dithiolene complex **4** as a dark solid. Data follow: yield = 93% (182 mg), mp >260 °C; ^1H NMR (300 MHz, DMSO-d_6) δ = 5.48 (s, 20H, Cp); HRMS (ESI) calculated for $C_{26}H_{20}S_8{}^{98}Mo_2$, 783.74389, found 783.7440.

DOI: 10.1021/acs.inorgchem.5b00632
Inorg. Chem. 2015, 54, 5013−5020

Synthesis of $Cp_2Ti(S_2TTF(SMe)_2)$ 5a. To a solution of TTF **1a** (209 mg, 0.45 mmol) in 25 mL of dry THF was slowly added, under argon, a freshly prepared solution of LDA (0.62 mL of *n*-BuLi 1.6 M in hexane, 0.14 mL of i-Pr_2NH in 4 mL of dry THF, 1 mmol). The solution was stirred 30 min at RT. Neat Cp_2TiCl_2 (125 mg, 0.5 mmol) was added, and the reaction was stirred overnight at RT. The reaction mixture was evaporated to dryness, extracted with CH_2Cl_2, and washed with water. After evaporation of the solvent under vacuum, the solid was purified by chromatography with CH_2Cl_2/PE (1/1) as eluent to afford **5a** as dark green solid. Slow concentration of a CH_2Cl_2/PE (1/1) solution of **5a** provided crystals suitable for X-ray diffraction analysis. Data follow for **5a**: yield = 30%, mp = 227 °C (dec); ^{1}H NMR (300 MHz, $CDCl_3$) δ = 2.42 (s, 6H, SCH_3), 5.73 (s, 5H, Cp), 6.04 (s, 5H, Cp); HRMS (ASAP) calculated for $C_{18}H_{16}S_8{}^{48}Ti$, 535.88492, found 535.8500.

Crystallography. Data were collected on an APEX II Bruker AXS diffractometer with graphite-monochromated Mo Kα radiation (λ = 0.710 73 Å). The structure were solved by direct methods using the *SIR97* program,[22] and then refined with full-matrix least-squares methods based on F^2 (*SHELXL-97*)[23] with the aid of the *WINGX* program.[24] All non-hydrogen atoms were refined with anisotropic atomic displacement parameters. H atoms were finally included in their calculated positions. Details of the final refinements are given in Table 4.

Table 4. Crystallographic Data for the Neutral Complex $Cp_2Mo(S_2TTF(SMe)_2)$ 2a, $Cp_2Ti(S_2TTF(SMe)_2)$ 5a, and the Salt [2a][I_3]

compound	2a	[2a][I_3]	5a
formula	$C_{18}H_{16}MoS_8$	$C_{18}H_{16}MoS_8$, I_3	$C_{18}H_{16}TiS_8$
fw (g mol^{-1})	584.73	965.43	536.69
cryst syst	monoclinic	triclinic	monoclinic
space group	$P2_1/n$	$P\bar{1}$	$P2_1/n$
a (Å)	10.9296(2)	7.5957(5)	7.6337(3)
b (Å)	18.2350(4)	13.3631(10)	12.0575(5)
c (Å)	11.1086(3)	14.3454(11)	23.2394(8)
α (deg)	90	68.822(2)	90
β (deg)	106.6580(10)	75.656(2)	93.266(2)
γ (deg)	90	87.366(2)	90
V (Å^3)	2121.04(8)	1313.89(17)	2135.56(14)
T (K)	150(2)	150(2)	150(2)
Z	4	2	4
D_{calc} (g cm^{-3})	1.831	2.44	1.669
μ (mm^{-1})	1.409	4.668	1.186
total reflns	17500	13258	18914
unique reflns (R_{int})	4869 (0.0341)	5974 (0.0382)	4863 (0.041)
unique reflns ($I > 2\sigma(I)$)	3893	4459	4175
R1, wR2	0.0459, 0.1031	0.0380, 0.0824	0.03590.0831
R1, wR2 (all data)	0.0617, 0.1093	0.0590, 0.0936	0.0434, 0.087
GOF	1.225	0.985	1.034

■ ASSOCIATED CONTENT

Supporting Information

Computational details and X-ray crystallographic files in CIF format. This material is available free of charge via the Internet at http://pubs.acs.org.

■ AUTHOR INFORMATION

Corresponding Author

*E-mail: dominique.lorcy@univ-rennes1.fr.

Notes

The authors declare no competing financial interest.

■ ACKNOWLEDGMENTS

The authors thank GENCI for allocation of computing time under Project c2015085032.

■ REFERENCES

(1) Special issue on "Dithiolenes and non-innocent redox-active ligands": *Coord. Chem. Rev.* **2010**, *13−14*, 1357−1588.

(2) (a) Cui, H.-B.; Kobayashi, H.; Ishibashi, S.; Sasa, M.; Iwase, F.; Kato, R.; Kobayashi, A. *J. Am. Chem. Soc.* **2014**, *136*, 7619−7622. (b) Zhou, B.; Idobata, Y.; Kobayashi, A.; Cui, H.; Kato, R.; Takagi, R.; Miyagawa, K.; Kanoda, K.; Kobayashi, H. *J. Am. Chem. Soc.* **2012**, *134*, 12724−12731. (c) Okano, Y.; Zhou, B.; Tanaka, H.; Adachi, T.; Ohishi, Y.; Takata, M.; Aoyagi, S.; Nishibori, E.; Sakata, M.; Kobayashi, A.; Kobayashi, H. *J. Am. Chem. Soc.* **2009**, *131*, 7169−7174. (d) Kobayashi, A.; Fujiwara, E.; Kobayashi, H. *Chem. Rev.* **2004**, *104*, 5243−5264. (e) Tanaka, H.; Okano, Y.; Kobayashi, H.; Suzuki, W.; Kobayashi, A. *Science* **2001**, *291*, 285−287.

(3) Matsubayashi, G.; Nakano, M.; Tamura, H. *Coord. Chem. Rev.* **2002**, *226*, 143−151.

(4) Schlueter, J. A. *Top. Organomet. Chem.* **2009**, *27*, 1−33.

(5) Eisenberg, R.; Gray, H. B. *Inorg. Chem.* **2011**, *50*, 9741−9751.

(6) (a) Mueller-Westerhoff, U. T.; Vance, B.; Yoon, D. I. *Tetrahedron* **1991**, *47*, 909−932. (b) Lim, B. S.; Fomitchev, D. V.; Holm, R. H. *Inorg. Chem.* **2001**, *40*, 4257−4262. (c) Szilagyi, R. K.; Lim, B. S.; Glaser, T.; Holm, R. H.; Hedman, B.; Hodgson, K. O.; Solomon, E. I. *J. Am. Chem. Soc.* **2003**, *125*, 9158−9169.

(7) McCullough, R. D.; Belot, J. A.; Seth, J.; Rheingold, A. L.; Yap, G. P. A.; Cowan, D. O. *J. Mater. Chem.* **1995**, *5*, 1581−1587.

(8) Saito, K.; Nakano, M.; Tamura, H.; Matsubayashi, G. *Inorg. Chem.* **2000**, *39*, 4815−4820.

(9) Saito, K.; Nakano, M.; Tamura, H.; Matsubayashi, G. *J. Organomet. Chem.* **2001**, *625*, 7−12.

(10) Guyon, F.; Lenoir, C.; Fourmigué, M.; Larsen, J.; Amaudrut, J. *Bull. Soc. Chim. Fr.* **1994**, *131*, 217−226.

(11) Eid, S.; Roisnel, T.; Lorcy, D. *J. Organomet. Chem.* **2008**, *693*, 2345−2350.

(12) Harris, H. A.; Kanis, D. R.; Dahl, L. F. *J. Am. Chem. Soc.* **1991**, *113*, 8602−8611.

(13) (a) Fourmigué, M. *Acc. Chem. Res.* **2004**, *37*, 179−186. (b) Fourmigué, M. *Coord. Chem. Rev.* **1998**, *178−180*, 823−864.

(14) (a) Taylor, A. J.; Davies, E. S.; Weinstein, J. A.; Sazanovich, I. V.; Bouganov, O. V.; Tikhomirov, S. A.; Towrie, M.; McMaster, J.; Garner, C. D. *Inorg. Chem.* **2012**, *51*, 13181−13194. (b) Whalley, A. W.; Blake, A. J.; Collison, D.; Davies, E. S.; Disley, H. J.; Helliwell, M.; McMaster, J.; Wilson, C.; Garner, C. D. *Dalton Trans.* **2011**, *40*, 10457−10472.

(15) (a) Swietlik, R.; Jankowski, D.; Fourmigué, M.; Yakushi, K. *Vib. Spectrosc.* **2011**, *55*, 195−200. (b) Swietlik, R.; Lapinski, A.; Fourmigué, M.; Yakushi, K. *J. Raman Spectrosc.* **2009**, *40*, 2092−2098. (c) Clérac, R.; Fourmigué, M.; Coulon, C. *J. Solid. State Chem.* **2001**, *159*, 413−419. (d) Domercq, B.; Coulon, C.; Fourmigué, M. *Inorg. Chem.* **2001**, *40*, 371−378. (e) Clerac, R.; Fourmigué, M.; Gaultier, J.; Barrans, Y.; Albouy, P. A.; Coulon, C. *Eur. Phys. J. B* **1999**, *9*, 431−443. (f) Clérac, R.; Fourmigué, M.; Gaultier, J.; Barrans, Y.; Albouy, P. A.; Coulon, C. *Eur. Phys. J. B* **1999**, *9*, 445−459. (g) Fourmigué, M.; Domercq, B.; Jourdain, I. V.; Molinié, P.; Guyon, F.; Amaudrut, J. *Chem.—Eur. J.* **1998**, *4*, 1714−1723. (h) Fourmigué, M.; Lenoir, C.; Coulon, C.; Guyon, F.; Amaudrut, J. *Inorg. Chem.* **1995**, *34*, 4979−4985.

(16) (a) Svenstrup, N.; Rasmussen, K. M.; Hansen, T. K.; Becher, J. *Synthesis* **1994**, 809−812. (b) Simonsen, K. B.; Svenstrup, N.; Lau, J.; Simonsen, O.; Mork, P.; Kristensen, G. J.; Becher, J. *Synthesis* **1996**, 407−418.

(17) (a) Vacher, A.; Barrière, F.; Roisnel, T.; Lorcy, D. *Chem. Commun.* **2009**, 7200−7202. (b) Vacher, A.; Barrière, F.; Roisnel, T.; Piekara-Sady, L.; Lorcy, D. *Organometallics* **2011**, *30*, 3570−3578. (c) Vacher, A.; Barrière, F.; Lorcy, D. *Organometallics* **2013**, *32*, 6130−6135.

DOI: 10.1021/acs.inorgchem.5b00632
Inorg. Chem. 2015, 54, 5013−5020

(18) Bsaibess, T.; Guerro, M.; Le Gal, Y.; Sarraf, D.; Bellec, N.; Fourmigué, M.; Barrière, F.; Dorcet, V.; Guizouarn, T.; Roisnel, T.; Lorcy, D. *Inorg. Chem.* **2013**, *52*, 2162−2173.
(19) Chappell, J. S.; Bloch, A. N.; Bryden, W. A.; Maxfield, M.; Poehler, T. O.; Cowan, D. O. *J. Am. Chem. Soc.* **1981**, *103*, 2442−2243.
(20) Reinheimer, E. W.; Zhao, H.; Dunbar, K. R. *Synth. Met.* **2008**, *158*, 447−452.
(21) Gao, F.; Zhu, F.-F.; Wang, X.-Y.; Xu, Y.; Wang, X.-P.; Zuo, J.-L. *Inorg. Chem.* **2014**, *53*, 5321−5327.
(22) Altomare, A.; Burla, M. C.; Camalli, M.; Cascarano, G.; Giacovazzo, C.; Guagliardi, A.; Moliterni, A. G. G.; Polidori, G.; Spagna, R. *J. Appl. Crystallogr.* **1999**, *32*, 115−119.
(23) Sheldrick, G. M. *Acta Crystallogr.* **2008**, *A64*, 112−122.
(24) Farrugia, L. J. *J. Appl. Crystallogr.* **2012**, *45*, 849−854.

DOI: 10.1021/acs.inorgchem.5b00632
Inorg. Chem. 2015, 54, 5013−5020